CMS Physics Analysis Summary

Contact: cms-pag-conveners-exotica@cern.ch 2012/07/10

Search for pair production of third generation leptoquarks and stops that decay to a tau and a b quark

The CMS Collaboration

Abstract

A search for third generation leptoquarks and stops using events from a data sample of pp collisions corresponding to an integrated luminosity of 4.8 fb^{-1}, collected by the CMS detector at the LHC with $\sqrt{s} = 7$ TeV is presented. The number of observed events containing two taus and two b jets is found to be in agreement with the standard model prediction. A 95% CL limit is set on the scalar (vector) leptoquark pair production cross section times β^2, where β is the branching fraction of leptoquark to a tau and a b quark. The third generation leptoquarks with masses below 525 GeV (for $\beta = 1$) and SU(5) vector leptoquarks with masses below 760 GeV are excluded at 95% CL. Limits are also set on the cross section for pair production of the supersymmetric partner of the top quark (stop) in R-parity violating supersymmetric scenario. Stops with masses below 453 GeV are excluded at 95% CL for a typical benchmark scenario, assuming coupling between stop, tau, and b quark, $\lambda'_{333} = 1$. Both of these results represent the most stringent mass limits on these particles to date. The stringent limits on λ'_{333} are also set excluding coupling values not ruled out by indirect bounds.

1 Introduction

Many extensions of the standard model (SM), such as SU(5) grand unification [1, 2], Pati-Salam SU(4) [3], composite models [4, 5], superstrings [6], and technicolor [7–9] predict new bosons, called leptoquarks (LQ), that carry color and both lepton and baryon quantum numbers. Leptoquarks decay to a quark and a lepton with a branching fraction (β) to a quark and a charged lepton that is model dependent. Stringent limits on flavor-changing neutral currents and other rare processes favour leptoquarks that couple to quarks and leptons within the same SM generation for LQ masses accessible to current colliders [5, 10].

The dominant pair production mechanisms for leptoquarks at energies and masses accessible at the Large Hadron Collider (LHC) for current integrated luminosities are gluon-gluon fusion and quark-antiquark annihilation. The cross section for these processes has been calculated to next-to-leading-order (NLO) in α_s [11], and is independent of the coupling between the leptoquark, the lepton, and the quark (λ), depending only on its mass and spin. Results obtained are interpreted in both scalar and vector leptoquark context.

Supersymmetry (SUSY) is an attractive extension of the SM because it can resolve the hierarchy problem [12] without unnatural fine-tuning, if the mass of the supersymmetric partner of the top quark (stop) is not too large [13, 14]. Supersymmetric models can also have a new conserved quantum number, R-parity (R_p) [15], that distinguishes SM and SUSY particles. If R_p is violated, supersymmetric particles can decay to final states containing standard model particles only. Searches for supersymmetry that assume the supersymmetric partners of the quarks have degenerate masses and conservation of R parity have been so far unsuccessful [16, 17]. However, the large mixing angle (θ) between the left-chiral and right-chiral stops ($\widetilde{\mathrm{t}}_{\mathrm{L}}$ and $\widetilde{\mathrm{t}}_{\mathrm{R}}$) due to the large top Yukawa coupling can produce two mass eigenstates, $\widetilde{\mathrm{t}}_1$ and $\widetilde{\mathrm{t}}_2$, with $M_{\widetilde{\mathrm{t}}_1} < M_{\widetilde{\mathrm{t}}_2}$. $M_{\widetilde{\mathrm{t}}_1}$ can be smaller than the masses of the other scalar SUSY particles. Such a scenario, with a light stop and R-parity violation, would still allieviate the hierarchy problem of SM and is not excluded by current searches.

At the LHC, a stop and an anti-stop pair can be produced via strong interactions. When the mass of the supersymmetric partner of the gluon and quarks, excluding top quark are large, the stop anti-stop pair production cross section is the same as for third generation scalar leptoquarks. The cross section also depends on the first generation squark mass and the stop mixing angle due to the loop-corrections, but contribution from these processes is less than two percent. Trilinear R-parity violating operators allow the lepton-number-violating decay $\widetilde{\mathrm{t}}_{\mathrm{L}} \to \tau\mathrm{b}$ [15] with a coupling λ'_{333}, resulting in the same signature as one considered for third generation leptoquarks, with similar kinematics.

In this note, a search for a pair-production of third generation leptoquarks or stops decaying to two taus and two b jets using pp collision data collected by the CMS experiment equivalent to 4.8 fb^{-1} of integrated luminosity is presented. One of the taus in the final state is required to decay leptonically: $\tau \to \ell\nu_\ell\nu_\tau$, where ℓ can be either a muon or an electron. The other tau (τ_h) is required to decay to hadrons: $\tau \to$ hadrons ν_τ. This requirement results in two independent final states referred to as $\mathrm{e}\tau_\mathrm{h}\mathrm{b}\overline{\mathrm{b}}$ and $\mu\tau_\mathrm{h}\mathrm{b}\overline{\mathrm{b}}$, respectively. The experimental signature is characterized by an energetic electron or muon, a τ_h, and two jets produced by the hadronization of b quarks (b jets). The scalar sum of the transverse momenta of the decay products, $S_\mathrm{T} \equiv p_\mathrm{T}^{\tau_\mathrm{h}} + p_\mathrm{T}^{\ell} + p_\mathrm{T}^{\mathrm{b}_1} + p_\mathrm{T}^{\mathrm{b}_2}$, is expected to be large for pair production of LQs or stops, and the tau and the bjet that originated from the same heavy particle are expected to have a large invariant mass.

Previous searches for leptoquarks were carried out at pp, p$\bar{\mathrm{p}}$, $\mathrm{e}^+\mathrm{e}^-$, and ep colliders [18–23].

The most stringent lower limit to date on the mass of a third generation leptoquarks in the final state with tau, lepton, and two bjets, assuming $\beta = 1$, is 210 GeV from the D0 experiment [19]. The most recent constraints on $\widetilde{t}_1\bar{\widetilde{t}}_1$ production in the final state with tau, lepton and two b jets come from the CDF experiment, using 322 pb^{-1} of data. A 95% CL upper limit of 153 GeV was placed on the $\widetilde{t}_1$ mass [24]. The indirect bounds exclude couplings between stop, tau and b quark, stronger than 0.26 [25] for $M_{\widetilde{t}_1} \sim 100$ GeV.

2 CMS detector

The central feature of the CMS apparatus is a superconducting solenoid, of 6 m internal diameter, providing a field of 3.8 T. Within the field volume are a silicon pixel and strip tracker, which allows the reconstruction of the trajectories of charged particles within the pseudorapidity range $|\eta| < 2.5$, where $\eta = -\ln\tan(\theta/2)$ and θ is the polar angle, and calorimetry system consisting of a lead tungstate crystal electromagnetic calorimeter (ECAL) and a brass/scintillator hadron calorimeter (HCAL), which measures particle energy depositions for $|\eta| < 3$. CMS also has extensive forward calorimetry. Muons are measured in gas-ionization detectors embedded in the steel return yoke. Collision events are selected using a two-tiered trigger system [26]. A more detailed description of CMS detector can be found in Ref. [27].

3 Trigger and event selection

Candidate LQ or stop events were collected using a set of triggers requiring the presence of two objects, a τ_h and an electron or a muon with transverse momentum thresholds ranging between 12-20 GeV depending on the data-taking period.

Electrons are reconstructed within the geometrical acceptance $|\eta| < 2.1$ using information from the ECAL and the tracker. Selected electrons are required to have transverse momenta $p_T >$ 30 Gev, an electromagntic shower shape consistent with that of an electron, and an energy deposition in ECAL that is compatible with the track reconstructed in the tracker. Muons are required to be reconstructed by both the tracker and the muon spectrometer. They are required to have $|\eta| < 2.1$ and $p_T > 30$ GeV. A particle-flow (PF) technique [28–30] is used for the reconstruction of hadronically decaying τ_h candidates. In the PF approach, information from all subdetectors is combined to reconstruct and identify all final-state particles produced in the collision. The particles are classified as either charged hadrons, neutral hadrons, electrons, muons, and photons. These particles are used with the hadron plus strip (HPS) algorithm [31] to identify τ_hs. Hadronic decays of taus with one or three charged pions and up to two neutral pions are reconstructed. The reconstructed τ_h is required to have $p_T > 50$ GeV and $|\eta| < 2.3$. Selected electrons, muons, and taus are required to be isolated from other reconstructed particle activities. The identified electron (muon) and τ_h are required to originate from the same vertex and be separated spatially by $\Delta R \equiv \sqrt{\Delta\phi^2 + \Delta\eta^2} > 0.5$. The lepton and the τ_h are also required to have opposite electric charge.

Jets are reconstructed with the anti-k_t algorithm with a distance parameter $R = 0.5$ [32, 33] using PF candidates. Jet energies are corrected by subtracting the average contribution from particles from other proton-proton collisions in the same beam crossing (pileup) and by correcting the jet momentum to better reflect the true total momentum of the particles in the jet [34]. Selected jets are required to be within $|\eta| < 2.4$ and have $p_T > 30$ GeV, and to be separated from the selected electron or muon and the τ_h by $\Delta R > 0.5$. The selected events are required to have at least two jets identified as originating from b-quark hadronization (b-tagged) using the track counting algorithm, based on the track impact parameter significance [35]. The p_T distribution of bjets is shown in Fig. 1.

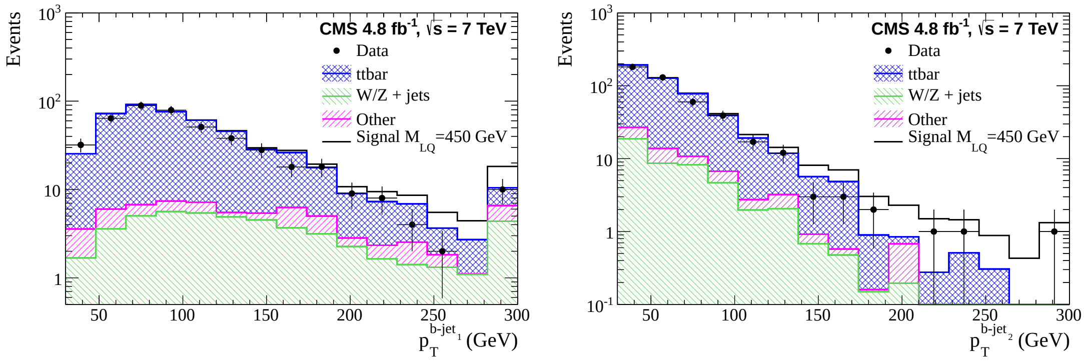

Figure 1: p_T distribution of the leading b-tagged jet (left) and second leading b-tagged jet (right) for data (black dots) and stacked SM backgrounds (color) and 450 GeV LQ signal (black line).

To discriminate between signal and background, the mass of the τ_h and b jet, ($M_{\tau_h,b}$), is required to be greater than 170 GeV (190 GeV) for signal hypotheses with masses up to 450 GeV (greater than 450 GeV). Of the two possible pairings of the tau and b jet (M_{τ_h,b_1} and M_{τ_h,b_2}), the one for which the the invariant mass is closest to the invariant mass of the lepton and the other b jet is chosen as an observable. Other possible pairings were found to have similar sensitivity. The S_T distribution after the final selection is used to extract the limit.

4 Event samples

The dominant sources of $\ell\tau_h b\bar{b}$ events from SM processes is pair production of top quarks and associated production of a W or Z boson with jets, where the jet is misidentified as a τ_h. There is also a small contribution from Z bosons decaying to a pair of taus, or to pairs of electrons or muons, when one of the electrons or muons is misidentified as the τ_h, and from single top, and diboson processes.

The signal is modeled using the PYTHIA v6.4 [36] generator for a range of leptoquark masses M_{LQ} spanning 200 to 650 GeV. We use the MADGRAPH generator [37] interfaced with TAUOLA [38] for tau lepton decay, and PYTHIA v6.4 for hadronization and showering, to model the dominant $t\bar{t}$ and W+jets backgrounds. These generators are also used to model the less significant Drell-Yan process $Z/\gamma^* \rightarrow \ell\ell$. The single top production is modeled with the POWHEG [39] generator interfaced with PYTHIA v6.4, and diboson processes are modeled with PYTHIA v6.4. All generated samples are passed through a full detector simulation based on GEANT4 [40] and the complete reconstruction chain used for the analysis of collision data. The NLO [11] and the next-to-next-to-leading order cross sections are used to normalize the signal and background processes [41–43], respectively.

Efficiencies of the trigger and final selection criteria for signal process are estimated from the simulation and corrected to match that observed in data during different data-taking periods. The trigger efficiency for signal events with a LQ mass hypothesis of 550 GeV is close to 90% for both channels. The efficiency of the final selection is 8.4% $\pm$ 0.2%(stat.) $\pm$ 0.6%(syst.) and 13.3% $\pm$ 0.3%(stat.) $\pm$ 0.9%(syst.) for $e\tau_h b\bar{b}$ and $\mu\tau_h b\bar{b}$ channels, respectively.

The top background is estimated using the simulated data. The normalization and several kinematic distributions of the top background are validated using events rejected by the $M_{\tau_h,b}$ >

170 GeV criterium. Both the yield from the simulation and the distribution of S_T agree well with the data observation (Fig. 2). Systematic uncertainties of 17% and 13% are assigned to the normalization of the $t\bar{t}$ background in $e\tau_h b\bar{b}$ and $\mu\tau_h b\bar{b}$ channels, respectively, based on the statistical uncertainties of the control sample and the uncertainties assigned to the MC prediction (Sec. 5) to which it is compared.

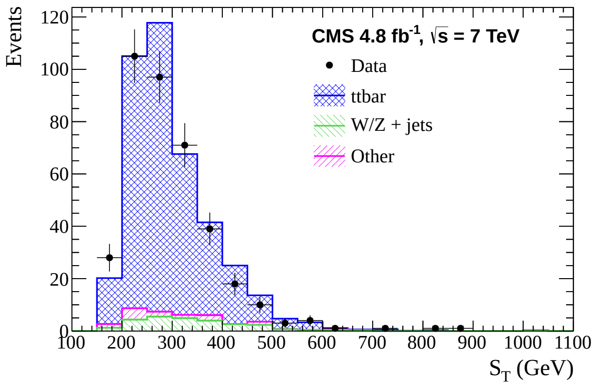

Figure 2: Stacked S_T distribution of the sample of events rejected by the $M_{\tau_h,b} > 170$ GeV selection. This control region is dominated by the top processes and is used to validate the level of the top background.

The number of background events containing a jet misidentified as a τ_h is estimated from data. The probability of misidentification is measured using events with a W boson produced in association with one jet passing loose τ_h identification that does not include the isolation requirement. The leptonic decay of the W boson is used. In the selected sample, the lepton is required to be well identified, and the transverse mass of the lepton and missing transverse energy, defined as

$$M_T = \sqrt{2 p_T^{\ell} \not{E}_T (1 - cos(\Delta\phi))}, \tag{1}$$

is required to be greater than 50 GeV. Here, p_T^{ℓ} and $\not{E}_T$ are transverse momentum of the lepton and imbalance of the transverse energy in the event, respectively, and $\Delta\phi$ is the azimuthal angle between the lepton and the $\not{E}_T$ direction. To reduce the contribution from $t\bar{t}$ events, the candidate τ_h and the lepton are required to have the same electric charge. The measured misidentification probability to pass the full τ_h requirements is independent of the transverse momentum and pseudorapidity of the candidate τ_h, and is $fr = 2.44\% \pm 0.53\%$. The number of background events is obtained using this misidentification probability and the number of events in a sample requiring a lepton, two bjets, and an additional jet passing the loose τ_h identification requirement but failing the isolation requirement. The lepton is required to satisfy the identification criteria used in the signal selection and the τ_h is required to have opposite electric charge to the lepton. The number of background events is calculated using the formula:

$$N_{bkg} = \frac{fr}{1 - fr} N_{anti-iso} \tag{2}$$

The S_T distribution for this background is determined using the simulated data. Because of statistical limitations on the existing MC samples, events with a lepton, a τ_h, and two jets were used, and the jet p_T spectrum is reweighted to match that expected from b jets. The difference in p_T spectra was obtained by comparing MC samples requiring only one jet and also by comparing samples with the lepton and τ_h required to have p_T below the values used to select the signal region.

The small backgrounds, $Z \rightarrow \tau\tau$ and diboson processes decaying to real τ_h, are estimated using the simulated data, as are the contributions from $Z \rightarrow ee$, and $Z \rightarrow \mu\mu$ processes, with an electron or a muon misidentified as a τ_h.

5 Systematic uncertainties

The background estimation as well as the signal selection efficiency could be affected by systematic uncertainties. The uncertainty on the total integrated luminosity is 2.2% [44]. The uncertainty assigned to the trigger and lepton efficiencies is 1-3%. The uncertainty on the τ_h identification efficiency is 6%, while the uncertainty on the b-tagging and mis-tagging efficiencies are 4% and 10%, respectively. The normalization uncertainties on the $t\bar{t}$, diboson, and $Z \rightarrow \tau\tau/\ell\ell$ are 13-17%, 30%, and 3.5%, respectively, due to the precision of their cross section measurements [45–47]. Due to the statistical limitation on $Z \rightarrow \tau\tau/\ell\ell$ simulation, the uncertainty on these backgrounds is 70% and 30% for the $e\tau_h$bb and $\mu\tau_h$bb respectively. Due to the misknowledge of the $Zb\bar{b}$ background in the phase space selected by the analysis, a 40% systematic uncertainty is assigned to the modelling of the $Zb\bar{b}$ background [48]. A 4% uncertainty is assigned to the signal acceptance due to modelling of initial and final state radiation in the simulation. The effect of pileup modelling in the MC is estimated to be on the order of 3%. Jet energy scale (2–4% depending on pseudorapidity and transverse momentum) as well as energy scale and resolution uncertainties for τ_hs (3%) which affects both the S_T distribution and the expected yields from the signal and background processes are taken into account.

Uncertainties due to the choice of parton distribution functions (PDF) of the proton lead to changes in the total cross section and the acceptance for both signal and background processes. PDF uncertainties on the signal theoretical cross section are calculated using the CTEQ6.6 PDF sets from [49], and vary from 19.5% to 28.1% depending on the mass hypothesis. Uncertainties on the detector acceptance have a negligible impact on both signal and background processes.

6 Results

The number of observed events and the expected signal and background yields after the final selection criteria $M_{\tau_h,b} > 170\,(190)$ GeV are listed in Table 1(Table 2). Data are in good agreement with the SM background prediction.

The $M_{\tau_h,b}$ and S_T distributions of selected events in data and MC simulation are shown in Fig. 3 and Fig. 4, respectively. As the distributions of S_T and $M_{\tau_h,b}$ observed in data are in good agreement with the SM background prediction, a limit is set on the third generation leptoquark pair-production cross section times β^2. The modified frequentist construction CL_s [50–52] is used for limit calculation and the $e\tau_h b\bar{b}$ and $\mu\tau_h b\bar{b}$ channels are combined, taking into account correlations between the systematic uncertainties. The limits as a function of mass are shown in Fig. 5 and the limits as a function of the leptoquark branching ratio β and the mass are shown in Fig. 6. Assuming $\beta = 1$, we exclude scalar leptoquarks with masses below 525 GeV, in good agreement with the expected limit at 543 GeV. The difference between vector and scalar LQ decay products kinematics is within a few percents for the used selection criteria. Thus, the results are interpreted as a search for vector leptoquarks predicted by SU(5) model [1, 2]. SU(5) vector leptoquarks with masses below 760 GeV are excluded that is in a good agreement with

	$\mu+\tau$ channel	$e+\tau$ channel
$t\bar{t}$	$38.1 \pm 3.4 \pm 4.9$	$10.9 \pm 1.8 \pm 1.4$
W+jets/Z+jets	$11.6 \pm 0.1 \pm 2.6$	$8.4 \pm 0.1 \pm 1.8$
$Z(\tau\tau/ll)$	$5.0 \pm 1.6 \pm 0.7$	$2.1 \pm 1.5 \pm 0.3$
diboson	$0.5 \pm 0.1 \pm 0.2$	$0.3 \pm 0.1 \pm 0.1$
Total Bkg.	$55.2 \pm 5.2 \pm 8.4$	$21.8 \pm 3.5 \pm 3.6$
Data	46	25
Signal (450 GeV)	$13.2 \pm 0.3 \pm 0.9$	$8.4 \pm 0.2 \pm 0.6$

Table 1: Estimated signal and background yields and observed data events after the final selection with $M_{\tau,b} > 170$ GeV requirement. The first uncertainty number corresponds to the statistical uncertainty and the second number to the systematic uncertainties on yield. PDF uncertainties are not included.

	$\mu+\tau$ channel	$e+\tau$ channel
$t\bar{t}$	$27.0 \pm 3.0 \pm 3.5$	$6.9 \pm 1.4 \pm 0.9$
W+jets/Z+jets	$9.1 \pm 0.1 \pm 2.0$	$7.2 \pm 0.1 \pm 1.6$
$Z(\tau\tau/ll)$	$5.0 \pm 1.6 \pm 0.7$	$2.1 \pm 1.5 \pm 0.3$
diboson	$0.4 \pm 0.1 \pm 0.1$	$0.2 \pm 0.1 \pm 0.1$
Total Bkg.	$41.5 \pm 4.8 \pm 6.3$	$16.4 \pm 3.1 \pm 2.9$
Data	36	17
Signal (500 GeV)	$6.75 \pm 0.14 \pm 0.45$	$4.37 \pm 0.11 \pm 0.29$
Signal (600 GeV)	$1.81 \pm 0.03 \pm 0.12$	$1.23 \pm 0.03 \pm 0.08$

Table 2: Estimated signal and background yields and observed data events after the final selection with $M_{\tau_h,b} > 190$ GeV requirement. The first uncertainty number corresponds to the statistical uncertainty and the second number to the systematic uncertainties on yield. PDF uncertainties are not included.

the expected limit at 762 GeV.

These results are also interpreted as a limit on R-parity violation stop production assuming massive SU(2) gaugino ($M_2 \geq 1$ TeV) which implies 100% branching fraction of the decay $\widetilde{t}_1 \rightarrow \tau b$. If $M_2 = 250$ GeV, $Br(\widetilde{t}_1 \rightarrow \tau b)$ decreases when the stop mass increases, as R-parity conserving decays open up. The limit on $\sigma \times Br(\widetilde{t}_1 \rightarrow \tau b)^2$ as a function of stop mass assuming $\lambda'_{333} = 1$, the higgsino mass $\mu = 380$ GeV, the ratio of higgs vacuum expectation values tanβ=40, and stop mixing angle $\theta = 0$, is also shown in Fig. 5. Using this benchmark, the R-parity violating stop is excluded for masses below 453 GeV in good agreement with expected exclusion at 474 GeV. The results are also interpreted as a of limit on RPV coupling λ'_{333} between stop, tau and bquark as a function of stop mass, as shown in Fig 6. The stops with masses below 240 GeV are excluded for all values of λ'_{333} coupling.

7 Conclusion

We performed a search for pair production of third generation scalar leptoquarks and supersymmetric partner of the top-quark with R-parity violation in the final state with an electron or muon, a hadronically-decaying tau, and two b jets. No excess above the SM background prediction is observed at high S_T. Therefore we exclude the existence of the scalar leptoquarks

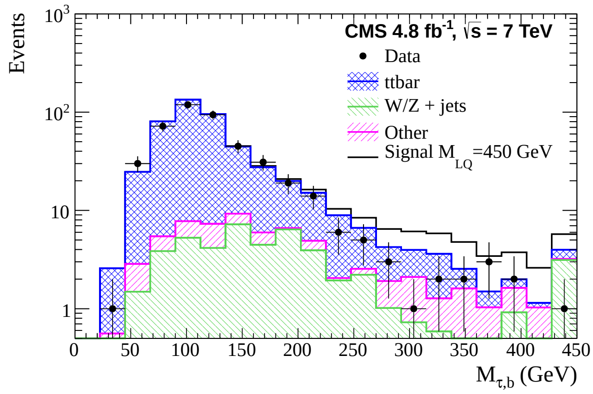

Figure 3: $M_{\tau_h,b}$ distribution for data (black dots) and the stacked SM backgrounds (colors) and 450 GeV LQ signal (black line) before applying the mass selection.

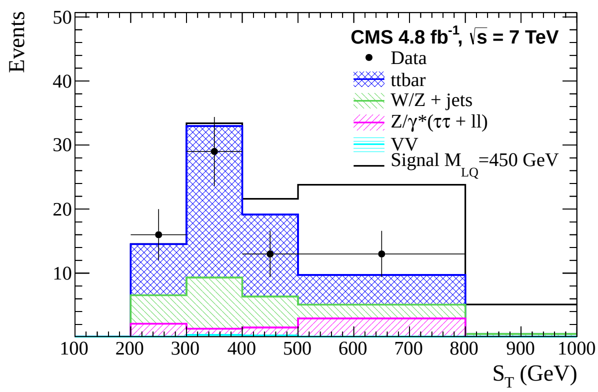

Figure 4: S_T distribution of data (black dots) and the stacked SM backgrounds (colors) and LQ signal (black line) after requiring $M_{\tau_h,b} > 170$ GeV. Uncertainty band reflects the statistical and systematic uncertainties on the SM processes.

with masses below 525 GeV assuming 100% branching ratio to a τ and a b quark at 95% CL. The SU(5) vector leptoquakrs with masses below 760 GeV are excluded at 95% CL. We also exclude stop with masses below 453 GeV for a given benchmark scenario and $\lambda'_{333} = 1$, and exclude stop masses below 240 GeV for any value of the λ'_{333} coupling. These limits are most stringent to date, and the limits on λ'_{333} coupling are the first direct limits that significantly improve previously-set indirect bounds.

We wish to congratulate our colleagues in the CERN accelerator departments for the excellent performance of the LHC machine. We thank the technical and administrative staff at CERN and other CMS institutes, and acknowledge support from: FMSR (Austria); FNRS and FWO (Belgium); CNPq, CAPES, FAPERJ, and FAPESP (Brazil); MES (Bulgaria); CERN; CAS, MoST, and NSFC (China); COLCIENCIAS (Colombia); MSES (Croatia); RPF (Cyprus); Academy of Sciences and NICPB (Estonia); Academy of Finland, ME, and HIP (Finland); CEA and CNRS/IN2P3 (France); BMBF, DFG, and HGF (Germany); GSRT (Greece); OTKA and NKTH (Hungary); DAE and DST (India); IPM (Iran); SFI (Ireland); INFN (Italy); NRF and WCU (Korea); LAS (Lithuania); CINVESTAV, CONACYT, SEP, and UASLP-FAI (Mexico); PAEC (Pakistan); SCSR (Poland); FCT (Portugal); JINR (Armenia, Belarus, Georgia, Ukraine, Uzbekistan); MST and MAE (Russia); MSTD (Serbia); MICINN and CPAN (Spain); Swiss

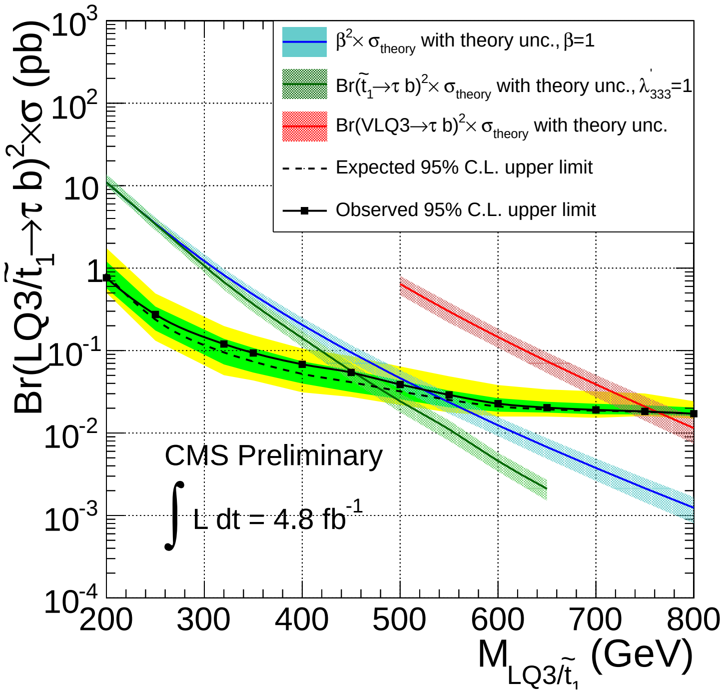

Figure 5: Expected and observed upper limit at 95% CL on the LQ ($\tilde{t}_1$) pair production cross section times $Br(LQ/\tilde{t}_1 \rightarrow \tau b)$ as a function of LQ ($\tilde{t}_1$) mass. The dark blue solid (dashed) curve and the light blue bands represent the theoretical LQ ($\tilde{t}_1$) pair production cross section and the uncertainties due to the choice of PDF and renormalization/factorization scales.

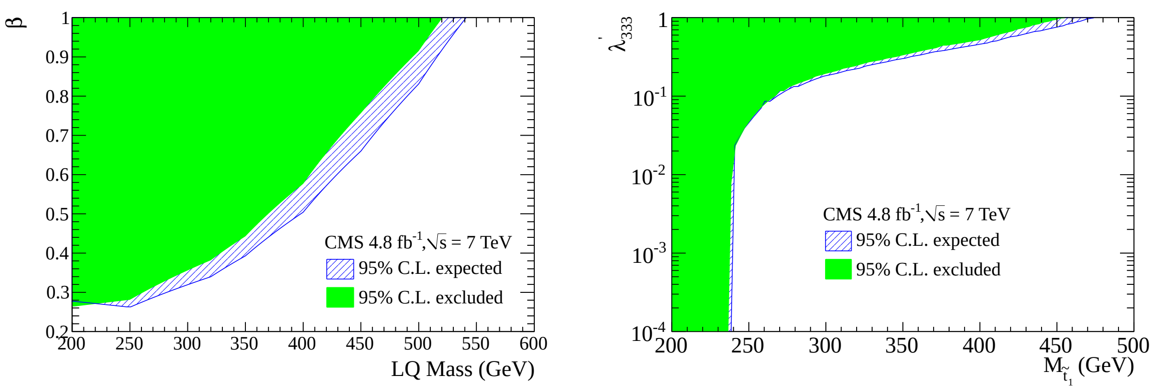

Figure 6: On the left: expected (blue dashed) and observed (green solid) 95% C.L. limit on the branching ratio beta between leptoquark and b quark plus tau lepton as a function of the leptoquark mass. On the right: expected (blue dashed) and observed (green solid) 95% C.L. limit on RPV coupling λ'_{333} between stop, tau, and b-quark.

Funding Agencies (Switzerland); NSC (Taipei); TUBITAK and TAEK (Turkey); STFC (United Kingdom); DOE and NSF (USA).

References

[1] H. Georgi and S. L. Glashow, “Unity of All Elementary-Particle Forces”, *Phys. Rev. Lett.* **32** (Feb, 1974) 438–441, doi:10.1103/PhysRevLett.32.438.

[2] S. Chakdar *et al.*, “Top SU(5) Model: Baryon and Lepton Number Violations at the TeV Scale”, (2012). arXiv:hep-ph/1206.0409.

[3] J. C. Pati and A. Salam, “Lepton number as the fourth ”color””, *Phys. Rev. D* **10** (Jul, 1974) 275–289, doi:10.1103/PhysRevD.10.275.

[4] B. Schrempp and F. Schrempp, “Light leptoquarks”, *Physics Letters B* **153** (1985), no. 12, 101 – 107, doi:10.1016/0370-2693(85)91450-9.

[5] W. Buchmüller and R. Rückl and D. Wyler, “Leptoquarks in lepton-quark collisions”, *Physics Letters B* **191** (1987), no. 4, 442 – 448, doi:10.1016/0370-2693(87)90637-X.

[6] J. L. Hewett and T. G. Rizzo, “Low-Energy Phenomenology of Superstring Inspired E(6) Models”, *Phys.Rept.* **183** (1989) 193, doi:10.1016/0370-1573(89)90071-9.

[7] S. Dimopoulos and L. Susskind, “Mass without scalars”, *Nuclear Physics B* **155** (1979), no. 1, 237 – 252, doi:10.1016/0550-3213(79)90364-X.

[8] S. Dimopoulos, “Technicoloured signatures”, *Nuclear Physics B* **168** (1980), no. 1, 69 – 92, doi:10.1016/0550-3213(80)90277-1.

[9] E. Eichten and K. Lane, “Dynamical breaking of weak interaction symmetries”, *Physics Letters B* **90** (1980), no. 12, 125 – 130, doi:10.1016/0370-2693(80)90065-9.

[10] O. Shanker, “pl3, kl3, and k0-k0bar constraints on leptoquarks and supersymmetric particles”, *Nuclear Physics B* **204** (1982), no. 3, 375 – 386, doi:10.1016/0550-3213(82)90196-1.

[11] M. Kramer *et al.*, “Pair production of scalar leptoquarks at the CERN LHC”, *Phys. Rev.* **D 71** (2005) 057503, doi:10.1103/PhysRevD.71.057503.

[12] S. P. Martin, “A Supersymmetry Primer”, (1997). arXiv:hep-ph/9709356. See also references therein.

[13] J. Wess and B. Zumino, “Supergauge transformations in four dimensions”, *Nuclear Physics B* **70** (1974), no. 1, 39 – 50, doi:10.1016/0550-3213(74)90355-1.

[14] H.-C. Cheng and I. Low, “TeV symmetry and the little hierarchy problem”, *JHEP* **0309** (2003) 051, doi:10.1088/1126-6708/2003/09/051.

[15] Barbier, R. and others , “R-Parity-violating supersymmetry”, *Physics Reports* **420** (2005), no. 16, 1 – 195, doi:10.1016/j.physrep.2005.08.006.

[16] C. Collaboration, “Search for supersymmetry in events with a lepton, a photon, and large missing transverse energy in pp collisions at sqrt(s) = 7 TeV”, *JHEP* **6** (2011) 93, doi:10.1007/JHEP06(2011)093.

[17] C. Collaboration, “Search for Supersymmetry at the LHC in Events with Jets and Missing Transverse Energy”, *Phys. Rev. Lett.* **107** (2011) 221804, doi:10.1103/PhysRevLett.107.221804.

[18] D0 Collaboration Collaboration, "Search for Third Generation Scalar Leptoquarks Decaying into τb", *Phys. Rev. Lett.* **101** (Dec, 2008) 241802, doi:10.1103/PhysRevLett.101.241802.

[19] D0 Collaboration Collaboration, "Search for Third-Generation Scalar Leptoquarks in $p\overline{p}$ Collisions at $\sqrt{s} = 1.96$ TeV", *Phys. Rev. Lett.* **99** (Aug, 2007) 061801, doi:10.1103/PhysRevLett.99.061801.

[20] (CDF Collaboration) Collaboration, "Search for Third Generation Leptoquarks in $\overline{p}p$ Collisions at $\sqrt{s} = 1.8$ *TeV*", *Phys. Rev. Lett.* **78** (Apr, 1997) 2906–2911, doi:10.1103/PhysRevLett.78.2906.

[21] CDF Collaboration Collaboration, "Search for third generation vector leptoquarks in $p\overline{p}$ collisions at $\sqrt{s} = 1.96$ TeV", *Phys. Rev. D* **77** (May, 2008) 091105, doi:10.1103/PhysRevD.77.091105.

[22] O. Collaboration, "Search for pair-produced leptoquarks in e^+e^- interactions at $\sqrt{s} \simeq 189$–209 GeV", *The European Physical Journal C - Particles and Fields* **31** (2003) 281–305. 10.1140/epjc/s2003-01325-y.

[23] CMS Collaboration, "Search for Pair Production of Third-Generation Scalar Leptoquarks Using Events Produced in pp Collisions at $\sqrt{s} = 7$ TeV Containing b-jets and Missing Transverse Energy",. CMS-PAS-EXO-11-030.

[24] CDF Collaboration Collaboration, "Search for Pair Production of Scalar Top Quarks Decaying to a τ Lepton and a b Quark in $p\overline{p}$ Collisions at $\sqrt{s} = 1.96$ TeV", *Phys. Rev. Lett.* **101** (Aug, 2008) 071802, doi:10.1103/PhysRevLett.101.071802.

[25] G. Bhattacharyya (1998). arXiv:hep-ph/9608415.

[26] CMS Collaboration, "The CMS high level trigger", *Eur. Phys. J. C* **46** (2006) 605, doi:10.1140/epjc/s2006-02495-8.

[27] CMS Collaboration, "The CMS experiment at the CERN LHC", *JINST* **3** (2008) S08004, doi:10.1088/1748-0221/3/08/S08004.

[28] CMS Collaboration, "Particle Flow Event Reconstruction in CMS and Performance for Jets, Taus, and MET". CMS PAS-PFT-09-001.

[29] CMS Collaboration, "Commissioning of the Particle-Flow Reconstruction in Minimum-Bias and Jet Events from pp Collisions at 7 TeV", CMS Physics Analysis Summary CMS-PAS-PFT-10-002, (2010).

[30] CMS Collaboration, "Commissioning of the particle-flow event reconstruction with leptons from J/Ψ and W decays at 7 TeV", CMS Physics Analysis Summary CMS-PAS-PFT-10-003, (2010).

[31] CMS Collaboration, "Performance of tau-lepton reconstruction and identification in CMS", *JINST* **7** (2012) 01001, doi:10.1088/1748-0221/7/01/P01001.

[32] G. P. Salam, "Towards Jetography", *Eur. Phys. J.* **C67** (2010) 637–686, doi:10.1140/epjc/s10052-010-1314-6.

[33] M. Cacciari, G. P. Salam, and G. Soyez, "The anti-k_T jet clustering algorithm", *JHEP* **04** (2008) 063, doi:10.1088/1126-6708/2008/04/063.

[34] C. Collaboration, "Determination of Jet Energy Calibration and Transverse Momentum Resolution in CMS", *JINST* **6** (2011) 11002, doi:10.1088/1748-0221/6/11/P11002.

[35] CMS Collaboration, "b-Jet identification in the CMS experiment", CMS Physics Analysis Summary CMS-PAS-BTV-11-004, (2011).

[36] T. Sjostrand, L. Lonnblad, S. Mrenna et al., "Pythia 6.3 physics and manual", arXiv:hep-ph/0308153.

[37] J. Alwall *et al.*, "MadGraph/MadEvent v4: The New Web Generation", *JHEP* **09** (2007) 028, doi:10.1088/1126-6708/2007/09/028.

[38] Z. Wąs, "TAUOLA the library for tau lepton decay, and KKMC/KORALB/KORALZ...status report", *Nucl. Phys. B, Proc. Suppl.* **98** (2001) 96, doi:10.1016/S0920-5632(01)01200-2.

[39] S. Frixione, P. Nason, C. Oleari, "Matching NLO QCD computations with parton shower simulations: the POWHEG method", *JHEP* **11** (2007) 070, doi:10.1088/1126-6708/2007/11/070.

[40] S. Agostinelli *et al.*, "Geant4 a simulation toolkit", *Nuclear Instruments and Methods in Physics Research Section A: Accelerators, Spectrometers, Detectors and Associated Equipment* **506** (2003), no. 3, 250 – 303, doi:10.1016/S0168-9002(03)01368-8.

[41] K. Melnikov and F. Petriello, "Electroweak gauge boson production at hadron colliders through O(alpha(s)**2)", *Phys. Rev.* **D 74** (2006) 114017, doi:10.1103/PhysRevD.74.114017.

[42] R. Kleiss and W. J. Stirling, "Top quark production at hadron colliders: Some usefulformulae", *Z. Phys.* **C 40** (1988) 419–423, doi:10.1007/BF01548856.

[43] CMS Collaboration, "Measurement of W^+W^- production and search for the Higgs boson in pp collisions at $\sqrt{s} = 7$ TeV", *Phys. Lett. B* **699** (2011) doi:10.1016/j.physletb.2011.03.056.

[44] CMS Collaboration, "Absolute Calibration of the Luminosity Measurement at CMS: Winter 2012 Update", (2012).

[45] CMS Collaboration, "Measurement of the WW, WZ and ZZ cross sections at CMS". CMS-PAS-EWK-11-010.

[46] CMS Collaboration Collaboration, "Measurement of the $t\bar{t}$ production cross section in pp collisions at 7 TeV in lepton + jets events using b-quark jet identification", *Phys. Rev. D* **84** (Nov, 2011) 092004, doi:10.1103/PhysRevD.84.092004.

[47] CMS Collaboration, "Update of the measurement of Drell-Yan cross section in pp Collisions at $\sqrt{s} = 7$ TeV with 1.1 fb $^{-1}$ of 2011 data". CMS-PAS-EWK-11-020.

[48] CMS Collaboration, "Measurement of the Z/γ^*+b-jet cross section in pp collisions at $\sqrt{s}$ = 7 TeV.", arXiv:1204.1643.

[49] M. Krämer, T. Plehn, M. Spira et al., "Pair production of scalar leptoquarks at the CERN LHC", *Phys. Rev. D* **71** (Mar, 2005) 057503, doi:10.1103/PhysRevD.71.057503.

[50] T. Junk, "Confidence level computation for combining searches with small statistics", *Nucl. Instrum. Meth. A* **434** (1999) 435, doi:10.1016/S0168-9002(99)00498-2.

[51] A. L. Read, “Modified frequentist analysis of search results (the CLs method)”, CERN Report CERN-OPEN-2000-005, (2000).

[52] ATLAS and CMS Collaborations, LHC Higgs Combination Group, “Procedure for the LHC Higgs boson search combination in Summer 2011”, ATL-PHYS-PUB/CMS NOTE 2011-11, 2011/005, (2011).